NOTES AND CORRESPONDENCE

A General Form of Kuo's Cumulus Parameterization

JOHN MOLINARI

Department of Atmospheric Science, State University of New York at Albany, Albany, NY 12222

4 February 1985 and 26 March 1985

ABSTRACT

A formulation of Kuo's cumulus parameterization is described which satisfies arbitrary vertical profiles of apparent heat source (Q_1) and apparent moisture sink (Q_2). The approach requires little calculation, and for a given Q_1 and Q_2, contains only one parameter, the partitioning of available moisture between storage and precipitation. The proposed method is tested in the prediction of a mesoscale convective complex and its advantages and limitations are discussed.

1. Introduction

The approach of Kuo (1974) for incorporating subgrid scale effects of cumulus convection has been widely used in numerical weather prediction models. One weakness of the approach has been its inability to reproduce observed vertical profiles of apparent heat source and apparent moisture sink (e.g., Song and Frank, 1983). In this note, a generalized approach is developed that satisfies arbitrary vertical profiles of heat and moisture sources and sinks. This general form eliminates the paradox present in earlier formulations of Kuo's method, for which grid-scale vertical advection of temperature appeared explicitly, while vertical advection of moisture appeared only in an integrated sense.

The resulting simplified procedure, which requires few calculations and contains only a single free parameter for a given Q_1 and Q_2, is tested in prediction of a mesoscale convective complex (MCC), and potential applications of the approach are discussed.

2. Procedure

The apparent heat source and apparent moisture sink (Yanai *et al.*, 1973) contain the combined influence of the subgrid scale sources of radiation, convection, and turbulent boundary layer fluxes. Because each physical process is usually computed separately in numerical models, it is desirable to define a convective apparent heat source Q_1' and convective moisture sink Q_2' as follows:

$$Q_1' = \pi\left(\frac{\partial\bar{\theta}}{\partial t} + \overline{\mathbf{v}\cdot\nabla_p\theta} + \bar{\omega}\frac{\partial\bar{\theta}}{\partial p}\right) - Q_R - g\frac{\partial F_H}{\partial p}$$

$$= L(c - e) - \pi\,\overline{\omega'\frac{\partial\theta'}{\partial p}} \qquad (1)$$

$$Q_2' = -L\left(\frac{\partial\bar{q}}{\partial t} + \overline{\mathbf{v}\cdot\nabla_p q} + \bar{\omega}\frac{\partial\bar{q}}{\partial p}\right) - g\frac{\partial F_q}{\partial p}$$

$$= L(c - e) + L\overline{\omega'\partial q'/\partial p} \qquad (2)$$

where the overbar represents an average over one grid area, F_H and F_q represent boundary layer turbulent fluxes of heat and moisture, respectively, and

$$\pi = c_p\left(\frac{p}{p_0}\right)^{R/c_p} \qquad (3)$$

is the Exner function. Other variables have their usual meaning. Q_1' and Q_2' satisfy

$$\frac{1}{g}\int_0^{p_s} Q_1' dp = \frac{1}{g}\int_0^{p_s} Q_2' dp = LP_0 \qquad (4)$$

where P_0 is the surface precipitation rate.

Without loss of generality, horizontal variations and nonconvective diabatic heating will be neglected until the following section. Forecast equations for potential temperature and specific humidity can then be written

$$\left(\frac{\partial\bar{\theta}}{\partial t}\right)_{1D} = -\bar{\omega}\frac{\partial\bar{\theta}}{\partial p} + L\pi^{-1}(c - e) - \overline{\omega'\partial\theta'/\partial p} \qquad (5)$$

$$\left(\frac{\partial\bar{q}}{\partial t}\right)_{1D} = -\bar{\omega}\frac{\partial\bar{q}}{\partial p} + e - c - \overline{\omega'\partial q'/\partial p}. \qquad (6)$$

In the approach of Kuo (1974), as modified by Kanamitsu (1975) and Krishnamurti *et al.* (1976), the combined effects of condensation and vertical eddy fluxes are represented as follows:

$$L\pi^{-1}(c - e) - \overline{\omega'\partial\theta'/\partial p} = gL\pi^{-1}(1 - b)I\frac{\alpha}{\int_{p_t}^{p_b}\alpha dp} \qquad (7a)$$

$$-\bar{\omega}\frac{\partial\bar{q}}{\partial p}+e-c-\overline{\omega'\partial q'/\partial p}=gbI\frac{\beta}{\int_{p_t}^{p_b}\beta dp} \tag{7b}$$

where

$$I=-\frac{1}{g}\int_{p_t}^{p_b}\bar{\omega}\frac{\partial\bar{q}}{\partial p}dp \tag{8}$$

is the rate of moisture accession at a grid point, b is the fraction of I which increases storage of water vapor, p_b and p_t are the pressures at cloud base and top, respectively, and

$$\alpha=\pi\left(\frac{\theta_c-\bar{\theta}}{\Delta\tau}+\bar{\omega}\frac{\partial\bar{\theta}}{\partial p}\right) \tag{9a}$$

$$\beta=\frac{q_c-\bar{q}}{\Delta\tau}. \tag{9b}$$

In Kuo's approach, the net moistening, which is the small difference between $-\bar{\omega}\partial\bar{q}/\partial p$ and subgrid scale drying, is parameterized, and thus the vertical advection of moisture no longer appears explicitly, but is absorbed into the moisture supply I. The conservation properties of the above approach are discussed by Kanamitsu (1975), Anthes (1977), and Molinari and Corsetti (1985; hereafter MC). Using (1), (2), and (7a,b), the convective sources and sinks for the Kuo scheme can be written

$$Q'_{1K}=gL(1-b)I\frac{\alpha}{\int_{p_t}^{p_b}\alpha dp} \tag{10a}$$

$$Q'_{2K}=-L\left(gbI\frac{\beta}{\int_{p_t}^{p_b}\beta dp}+\bar{\omega}\frac{\partial\bar{q}}{\partial p}\right). \tag{10b}$$

In the current approach, α and β will be redefined such that Q'_{1K} and Q'_{2K} exactly satisfy arbitrary vertical distributions Q'_1 and Q'_2, i.e.,

$$Q'_{1K}\Big/\int_{p_t}^{p_b}Q'_{1K}dp=Q'_1\Big/\int_{p_t}^{p_b}Q'_1dp, \tag{11a}$$

$$Q'_{2K}\Big/\int_{p_t}^{p_b}Q'_{2K}dp=Q'_2\Big/\int_{p_t}^{p_b}Q'_2dp. \tag{11b}$$

Using (8) and (10), this requires

$$\alpha=Q'_1, \tag{12a}$$

$$\frac{\beta}{\int_{p_t}^{p_b}\beta dp}=\frac{1}{b}\frac{\gamma}{\int_{p_t}^{p_b}\gamma dp}-\frac{1-b}{b}\frac{Q'_2}{\int_{p_t}^{p_b}Q'_2dp}, \tag{12b}$$

where

$$\gamma=-\bar{\omega}\frac{\partial\bar{q}}{\partial p}, \tag{12c}$$

and (5)–(6) can be written, using (7), (8), and (12), as

$$\left(\frac{\partial\bar{\theta}}{\partial t}\right)_{1D}=-\bar{\omega}\frac{\partial\bar{\theta}}{\partial p}+gL\pi^{-1}(1-b)I\frac{Q'_1}{\int_{p_t}^{p_b}Q'_1dp} \tag{13}$$

$$\left(\frac{\partial\bar{q}}{\partial t}\right)_{1D}=-\bar{\omega}\frac{\partial\bar{q}}{\partial p}-g(1-b)I\frac{Q'_2}{\int_{p_t}^{p_b}Q'_2dp}. \tag{14}$$

Equation (13) is given by Anthes (1977) for an arbitrary heating distribution. Equation (14) explicitly contains the grid scale moistening implicit in the right-hand side of (7b), and expresses the moisture change in terms of the convective apparent moisture sink Q'_2. Equations (13)–(14) satisfy integral constraints of the Kuo scheme for any Q'_1 and Q'_2 (e.g., see MC). These two equations make up a very simple cumulus parameterization scheme which has the following properties:

(i) The shape of the vertical profiles of Q'_1 and Q'_2 are exactly reproduced, thus providing a link with diagnostic studies.

(ii) The magnitudes of Q'_1 and Q'_2 are still determined by Kuo's procedure, i.e., precipitation rate remains proportional to the instantaneous moisture supply on the grid.

(iii) For a given Q'_1 and Q'_2, only the moisture supply I must be computed, and the number of parameters is reduced to one: the moisture partitioning parameter b. Other calculations are needed to determine when to initiate convection (see below).

(iv) The inconvenience of having two forms of the moisture equation in the Kuo scheme, one with and one without convection (differing in the absence or presence of the vertical advection term), is eliminated. When convection is not active, the second right-hand side terms of (13)–(14) are omitted.

In three dimensions, the large-scale and diabatic terms missing in (13)–(14) are simply added:

$$\frac{\partial\bar{\theta}}{\partial t}=-\bar{\mathbf{v}}\cdot\nabla_p\bar{\theta}-\bar{\omega}\frac{\partial\bar{\theta}}{\partial p}+H_c+H_s+H_R+g\partial F_H/\partial p \tag{15}$$

$$\frac{\partial\bar{q}}{\partial t}=-\bar{\mathbf{v}}\cdot\nabla_p\bar{q}-\bar{\omega}\frac{\partial\bar{q}}{\partial p}-Q_c-P_s+g\partial F_q/\partial p \tag{16}$$

where supersaturation heating H_s and precipitation P_s are computed following Kanamitsu (1975; see MC for details), H_R is radiative heating, and

$$H_c=gL\pi^{-1}(1-b)I\frac{Q'_1}{\int_{p_t}^{p_b}Q'_1dp} \tag{17}$$

$$Q_c = g(1 - b)I \frac{Q'_2}{\int_{p_t}^{p_b} Q'_2 dp} \tag{18}$$

Convection is activated if all of the following conditions hold:

(i) The moisture supply is positive. This is a fundamental aspect of the Kuo approach.
(ii) The column is conditionally unstable and cloud top (determined by the level of vanishing temperature excess of an entraining cloud element) is at or above 650 mb. This eliminates shallow convection, which is generally not driven by moisture convergence and is not addressed by the Kuo approach.
(iii) Rising motion exists at cloud base.
(iv) Relative humidity exceeds a critical value, taken here as 0.8, at or one level above cloud base.

As a result of its simplicity, the approach has a number of limitations as well:

(i) Q'_1 and Q'_2 must be known, but in nature they vary in time (Houze, 1982) and space.
(ii) Cloud base must be defined as the first level at which the specified heat source and moisture sink are nonzero.
(iii) Unlike the more traditional Kuo scheme, the method does not necessarily force the grid scale toward a realistic profile such as that represented by T_c and q_c. If Q'_1 and Q'_2 are not consistently determined (i.e., from the same data set), the sounding in the model could evolve in an unrealistic manner.
(iv) The approach does not produce a smooth transition to a moist neutral state (Kanamitsu, 1975; Molinari and Corsetti, 1985), in that, as neutrality is approached, a discrepancy exists between the specified Q'_1 and Q'_2 and those for a saturated moist neutral atmosphere.

The above limitations will be addressed in the results presented below.

3. MCC Case Study

The approach will be tested on the MCC described by Bosart and Sanders (1981). Molinari and Corsetti showed that prediction of the MCC was greatly improved by inclusion of cumulus and mesoscale downdrafts in the limiting state in their approach (i.e., θ_c and q_c in Eq. 9). Several integrations will be performed using the current procedure which vary only in the choice of apparent heat source and moisture sink. Q'_1 and Q'_2 are defined: (a) as their mean values in the heavy rain region during the first three hours of the previous forecast of MC; (b) from Yanai *et al.* (1973); and (c) following Johnson (1984), but assuming that mesoscale rainfall makes up 40 percent of the total. In the final two experiments, Q'_1 and Q'_2 are mismatched to examine the sensitivity of the results to the consistency of the heat and moisture sources and sinks.

The equations, finite differencing, and physics of the primitive equation model are described by Molinari (1982a) and MC. The integration is carried out on a one degree latitude–longitude mesh over a 20 degree longitude by 12 degree latitude area, with 100 mb vertical resolution, and is identical to the previous integration except that (17)–(18) define the convective parameterization. As in MC, the b parameter is vertical-shear dependent, following Fritsch and Chappell (1980).

The first integration uses the mean Q'_1 and Q'_2 from MC shown in Fig. 1. The predicted 12-hour precipitation volume and maximum grid point value (see Table 1) are comparable in accuracy to those obtained by MC. Figures 2 and 3 show the evolution of saturated equivalent potential temperature (θ_{es}) and vertical motion over five hours at the same grid point shown by MC. The θ_{es} profile shows strong low-level cooling (except slight warming during the last hour), middle and upper level warming initially, and upper level cooling later in the period. The vertical motion profile shows a life cycle behavior similar to that in MC, with a shift to upper levels in the maximum vertical motion; a mesoscale updraft–downdraft couplet (Houze, 1982) evolves by the last hour shown, with saturated ascent in the upper troposphere and unsaturated descent with evaporation in the lower troposphere (evaporation alone is allowed to moisten only to 90 percent of saturation). The results contain many of the characteristics of the integration of MC, despite the vastly simpler formulation. The evolution of stability is reasonable, even though the heat source and moisture sink profiles do not depend on the evolving thermodynamic structure.

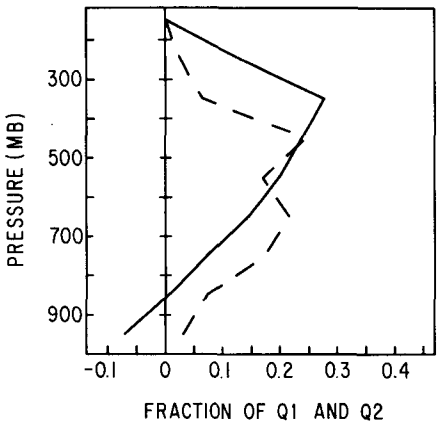

FIG. 1. Fraction of Q'_1 and Q'_2 in each 100 mb layer ($Q'_k \Delta p_k / \sum_k Q'_k \Delta p_k$) from the MCC simulation of Molinari and Corsetti (1985) with both cumulus and mesoscale downdrafts incorporated.

TABLE 1. Total rain volume (10^{12} kg) and maximum rainfall amount at a grid point (cm) over 12 hours for the MCC, computed from observations (Bosart and Sanders, 1981) and predicted for the various Q_1' and Q_2' profiles.

Heating/moistening profiles	Rain volume	R_{max}
Observed	2.15	2.9*
Time-dependent Q_1' and Q_2' (MC)	2.41	3.4
Q_1', Q_2' from Fig. 1	2.29	4.5
Q_1', Q_2' from Fig. 4b ($f = 0.4$)	1.44	2.4
Q_1', Q_2' from Fig. 4a ($f = 0.2$)	2.65	10.6
Q_1' for $f = 0.2$, Q_2' for $f = 0.3$	3.32	14.1
Q_1' for $f = 0.2$, Q_2' for $f = 0.4$	11.35	35.5

* Maximum point value >6 cm.

Although one dimensional integrations with fixed vertical motion reach a saturated moist neutral state (Molinari, 1982b), the process does not occur in three-dimensional integrations, despite the heavy precipitation in the MCC. Instead, convection is cut off because low-level cooling eventually stabilizes the column, or because lower tropospheric downdrafts develop and cause the moisture supply to become negative. In either case, convective activity stops well prior to the development of saturated moist neutrality, both in these integrations and those of MC, for which entraining updraft buoyancy played more of a direct role. The model behavior is consistent with the rarity of area-averaged saturation in observed precipitating convection. Because a saturated moist neutral state is never reached during active convection in the model, the discrepancy in the heating and moistening profiles during convectively driven evolution to moist neutrality appears not to be a problem.

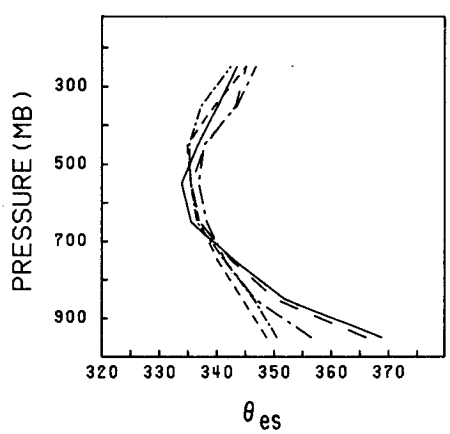

FIG. 2. Saturated equivalent potential temperature (K) at the grid point of heaviest precipitation for hours 2 (solid), 3 (large dash), 4 (large dash-dot), 5 (small dash), and 6 (small dash-dot) of the integration with Q_1' and Q_2' from Fig. 1.

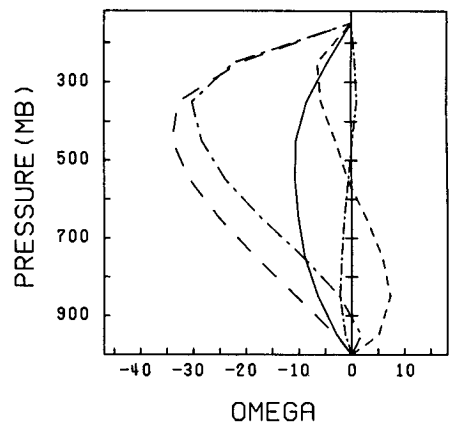

FIG. 3. Vertical velocity (μb s^{-1}) at the same point as Fig. 2 at hours 2 (small dash-dot), 3 (solid), 4 (large dash), 5 (large dash-dot), and 6 (small dash).

The remaining integrations define Q_1' and Q_2' based on the work of Johnson (1984), who determined the vertical profiles of cumulus scale heating and moistening as a residual from his mesoscale heating profiles and the Q_1 and Q_2 of Yanai *et al.* (1973). Johnson found that a fraction f of mesoscale rainfall of 0.2 produced the most realistic cumulus heating profile. Profiles for $f = 0.4$ are generated for this study assuming that the vertical structures of the cumulus and mesoscale components found by Johnson are universal, while the total Q_1 and Q_2 vary with the percentage of mesoscale precipitation. Following Johnson,

$$\hat{Q}_1 = f\hat{Q}_{1M} + (1-f)\hat{Q}_{1c} + Q_{Re}/P_0$$

$$\hat{Q}_2 = f\hat{Q}_{2M} + (1-f)\hat{Q}_{2c}$$

where the carat represents values normalized by the rainfall rate, subscript c is cumulus scale, M is mesoscale, and $\hat{Q}_{1M}$, $\hat{Q}_{1c}$, $\hat{Q}_{2M}$ and $\hat{Q}_{2c}$ are determined by tabulating Johnson's Figs. 7 and 8 and dividing by f (for cumulus) or $1-f$ (mesoscale). The resultant Q_1' and Q_2' profiles are shown in Fig. 4. The larger fraction of mesoscale precipitation strongly shifts the heating and drying to the upper troposphere.

Table 1 shows the predicted precipitation volume for $f = 0.2$ and $f = 0.4$. The former behaves similarly to the "no downdraft" integration of MC. Because low-level cooling is not present to stabilize the grid scale, a vigorous localized circulation develops and the model overpredicts the maximum precipitation. Conversely, the integration with mesoscale rainfall as 40 percent of the total stabilizes much more rapidly and significantly underpredicts rainfall amounts.

In order to evaluate the importance of consistency between Q_1' and Q_2', two additional integrations were carried out. In the first, Q_1' is derived using $f = 0.2$ and Q_2' using $f = 0.3$ (this does not violate energy or mass conservation because only the shape of the vertical

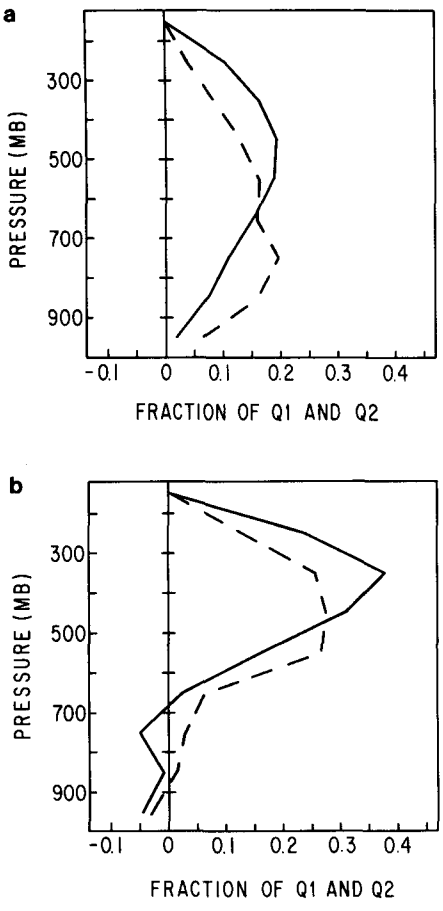

FIG. 4. (a) Fraction of Q'_1 and Q'_2 in each layer, assuming mesoscale rainfall makes up 20 percent of the total (Yanai *et al.*, 1973; Johnson, 1984). (b) As in (a) but with mesoscale rainfall as 40 percent of the total.

profiles is affected; see MC). This combination produces too much moistening below and too little aloft for the given heating. Table 1 shows that precipitation is strongly overpredicted. The Q'_1 profile destabilizes as earlier, but in this experiment Q'_2 contributes much more low level moistening, and thus increases the moisture available for convection and enhances the feedback instability. An additional integration with $f = 0.4$ in Q'_2 shows even greater overprediction of rainfall (Table 1). The occurrence of this instability depends not only on the heating profile, but also on the downward moisture flux implied by the Q'_1 and Q'_2 profiles of the latter two integrations. The presence of downward moisture flux is somewhat unlikely, and its addition to such a highly unstable situation represents an extreme case of possible instability due to the choice of Q'_1 and Q'_2. Nevertheless, the results indicate the dangers of significant inconsistencies in the specified heat source and moisture sink, which are most appropriately obtained from the same data set.

4. Discussion and conclusions

A fundamental goal of research into cumulus convection remains the understanding of the interaction and mutual intensification of the cumulus scale and larger scales of motion. The question cannot be addressed directly using a meso-α scale model (grid spacing 50–250 km), such as that used in this study, but only with a model whose scale is fine enough to resolve important aspects of the interaction, for example, the cumulus ensemble model of Soong and Ogura (1980). For meso-α scale models, the goal is simply to incorporate the unresolvable subgrid scale sources and sinks of heat and moisture (and momentum, which is not addressed in this work). Because these sources and sinks vary according to the dynamic and thermodynamic environment, the current approach, for which Q'_1 and Q'_2 must be known *a priori*, is limited in its application. Nevertheless, the approach has the significant benefits of simplicity and the ability to reproduce the shape of any desired profiles. Although the results were sensitive to large mismatches of the heat source and moisture sink, the approach performed nearly as well as a more complex procedure given reasonable Q'_1 and Q'_2. Its simplicity and flexibility may make it suitable for operational models, for which mean vertical profiles could be constructed as a function of latitude and/or season.

In a research framework, the method provides a straightforward means for testing the role of the vertical profiles of heating and moistening for various disturbances. In this study of an MCC, the most accurate rainfall prediction occurred when low-level cooling was present, but assuming that 40 percent of the rainfall fell in mesoscale downdrafts overestimated the low-level stabilization and underpredicted the rainfall.

Johnson (1984) has proposed that knowledge of the time dependence of the fraction of mesoscale rainfall within a convective cluster would allow construction of time-dependent Q'_1 and Q'_2 profiles which could be used in the Kuo framework. Equations (17)–(18) allow this time dependence to be incorporated easily, at the cost of additional parameters to be defined. The performance of fixed and time-dependent heat source and moisture sink profiles will be compared to that of more complex approaches in three-dimensional prediction experiments and will be reported on at a later time.

Acknowledgments. The manuscript was typed by Kathy Stutsrim. This research is supported by NSF Grant ATM-8317104.

REFERENCES

Anthes, R. A., 1977: A cumulus parameterization scheme utilizing a one-dimensional cloud model. *Mon. Wea. Rev.*, **105**, 270–286.

Bosart, L. F., and F. Sanders, 1981: The Johnstown flood of July

1977: A long-lived convective system. *J. Atmos. Sci.*, **38,** 1616–1642.

Fritsch, J. M., and C. F. Chappell, 1980: Numerical prediction of convectively driven mesoscale pressure systems. Part I: convective parameterization. *J. Atmos. Sci.*, **37,** 1722–1733.

Houze, R. A., Jr., 1982: Cloud clusters and large-scale vertical motions in the tropics. *J. Meteor. Soc. Japan,* **60,** 396–410.

Johnson, R. H., 1984: Partitioning tropical heat and moisture budgets into cumulus and mesoscale components: Implications for cumulus parameterization. *Mon. Wea. Rev.*, **112,** 1590–1601.

Kanamitsu, M., 1975: On numerical prediction over a global tropical belt. Ph.D. thesis, Dept. of Meteor., Florida State University, Tallahassee, FL 32304, 281 pp.

Krishnamurti, T. N., M. Kanamitsu, R. Godbole, C. B. Chang, F. Carr and J. Chow, 1976: Study of a monsoon depression (II), Dynamical structure. *J. Meteor. Soc. Japan,* **54,** 208–225.

Kuo, H. L., 1974: Further studies of the parameterization of the influence of cumulus convection on large scale flow. *J. Atmos. Sci.*, **31,** 1232–1240.

Molinari, J., 1982a: Numerical hurricane prediction using assimilation of remotely-sensed rainfall rates. *Mon. Wea. Rev.*, **110,** 553–571.

——, 1982b: A method for calculating the effects of deep cumulus convection in numerical models. *Mon. Wea. Rev.*, **110,** 1527–1534.

——, and T. Corsetti, 1985: Incorporation of cloud-scale and mesoscale downdrafts into a cumulus parameterization: Results of one- and three-dimensional integrations. *Mon. Wea. Rev.*, **113,** 485–501.

Song, J., and W. M. Frank, 1983: Relationships between deep convection and large-scale processes during GATE. *Mon. Wea. Rev.*, **111,** 2145–2160.

Soong, S.-T., and Y. Ogura, 1980: Response of tradewind cumuli to large-scale processes. *J. Atmos. Sci.*, **37,** 2035–2050.

Yanai, M., S. Esbensen and J. Chu, 1973: Determination of bulk properties of tropical cloud clusters from large-scale heat and moisture budgets. *J. Atmos. Sci.*, **30,** 611, 627.